X-ray Scattering from Nonideal CZ Silicon Crystals for High Energy Synchrotron Radiation

Hitoshi YAMAOKA[1], Shunji GOTO[2], Yoshiki KOHMURA[1], Tomoya URUGA[2] and Masahisa ITO[3]

1)The Institute of Physical and Chemical Research (RIKEN), Kamigori-cho, Ako-gun, Hyogo 678-12, Japan
2)The Japan Synchrotron Radiation Research Institute (JASRI), Kamigori-cho, Ako-gun, Hyogo 678-12, Japan
3)Himeji Institute of Technology (HIT), Kamigori-cho, Ako-gun, Hyogo 678-12, Japan

1. Introduction

In the SPring-8 incident beam energies of 100-150 keV will be used for high resolution experiments and 300 keV for magnetic Compton experiments. Energy spreads, $\delta E/E$, of 10^{-3} for 100-150 keV and 5×10^{-3} for 300 keV are required, where E is incident energy. The energy spread is too narrow especially for high energy x-rays of more than 100 keV compared to the mentioned required energy spread. Here we study mosaic silicon crystals for use as monochromators for high energy synchrotron radiation[1]. Study of mosaic crystals is also interesting from a physical view point when we consider the distortion mechanisms of mosaic crystals and the origin of diffuse scattering.

2. Samples

We prepared six kinds of mosaic crystals and one perfect crystal as samples taken from the same ingot crystal. A Czochralski-grown (CZ) dislocation-free Si 100 single crystal containing about 20 ppm oxygen as an impurity was used. Three of crystal samples were annealed at 780ºC for 24 hs, 1000ºC for 12 hs and 1170ºC for 12 hs. Pre-annealing at 780ºC for 24 hs was performed for the crystals annealed at 1000ºC and 1170ºC. The other three mosaic crystals were lapped, with mean abrasive particle sizes of 13 μm (No. 2000), 25 μm (No. 1000) and 42 μm (No. 600). One perfect crystal was also prepared as a sample for comparison.

3. Double- and triple-crystal diffractometry

First characterization was performed for six sample crystals and one perfect crystal in parallel (+, -) double-crystal arrangement in the Bragg case by measurement of rocking curves for Si 400. A Mo Kα line (17.5 keV) from a Mo rotating-anode x-ray generator was used. Experiments with triple-crystal diffractometry were performed at the BL14B of the Photon Factory. The incident energy for the sample crystal was 60 keV. The three Si 400 crystals were set in parallel (+n, -n, +n) arrangement of the Bragg case for simulation of the monochromator in the SPring-8 wiggler beam line. Physically the wave vectors, q_x and q_y in the reciprocal lattice space, correspond to lattice parameter fluctuation due to strain and lattice plane tilt or so-called mosaic spread, respectively. The directions of q_x and q_y correspond to [100] and [011], respectively. The reciprocal lattice vector $\mathbf{h}\{400\}$ is oriented in the direction of [100].

4. Results

The results from double-crystal diffractometry at 17.5 keV for annealed, lapped and perfect crystals are summarized in Table I. For the crystal annealed at 1000ºC for 12 hs after pre-annealing for 24 hs at 780ºC, the peak reflectivity is decreased and the integrated intensity is increased compared to those for the crystal annealed for 24 hs at 780ºC. In contrast, for the one annealed at 1170ºC the integrated intensity is increased and the peak reflectivity is not significantly different from that for the one annealed for 24 hs at 780ºC. For the lapped crystals, with increasing abrasive particle size, the reflectivity decreases and the integrated intensity increases monotonously. Figures 1 and 2 show contour maps of diffuse scattering from annealed and lapped crystals in the reciprocal lattice space, respectively. The data were taken by the triple-crystal diffractometry. The upper and lower panels show the symmetrical part and antisymmetrical part, respectively. On the map for the crystals annealed at 780ºC and 1000ºC in Fig. 1 the mosaic spread and lattice plane tilt can be seen to spread isotropically. But for the crystal annealed at 1170ºC the contour is narrower and the mosaic spread at larger q_x is changed dramatically compared to those for the crystals annealed at the lower temperatures. The antisymmetrical parts are very similar for these three annealed samples. The antisymmetrical profiles have angles with respect to the q_x axis by an asymmetrical angle of a. In Fig. 2 the symmetrical parts are similar for the three lapped samples. As for the antisymmetrical part, especially for the crystals lapped with the No. 600 and No. 1000 particles, these crystals have very different distributions compared to those for the annealed crystals. However we cannot find a theory of distorted crystals by the defects that can explain such a distribution.

5. Discussion

The advantage of using the crystal annealed at 1170ºC is small because the differences in the intensity and the energy spread are small compared to those for the other crystals and it is not easy to anneal a crystal at such a high temperature. The crystal lapped with the No. 600 particles is not suitable for use because it is slightly wider than required. From the fact that extinctions occur, the effective depth which contributes to the diffuse scattering is much smaller than the absorption depth in the Bragg case and the two methods, the lapping and the annealing, gave comparable effects on the diffuse scattering in the experiment. We would expect the same effect for a photon energy of 100-150 keV because the effective depth is considered not to depend on the incident energy strongly in the Bragg case. The diffuse scattering intensities of the annealed crystals show strong annealing temperature dependence. There is critical temperature for the production of defect between 1000ºC and 1170ºC. On the other hand, the slope of the profile for the lapped crystals does not depend on the lapping particle size. This indicates that the physical mechanisms of disordering of the crystal lattice plane by lapping may be almost the same for all abrasive particle sizes although the integrated intensity increases with the abrasive particle size. For lapped crystals, it was considered that the misorientation was the main reason for the increase in FWHM of the rocking curve. However our results suggest that lattice parameter fluctuations are also an origin of the broadening.

Reference

[1] H. Yamaoka et al. Jpn. J. Appl. Phys. **36** (1997) to be published.

Table I Sample crystals used in the experiments with measured rocking curve width, reflectivity, relative integrated intensity and resolution at 17.5 keV.

sample no.	sample name	species	resistivity (Wcm)	O_2 impurity (ppm)	carbon impurity (ppm)	rocking curve width (arcsec)	reflectivity (%)	relative integrated intensity	$\delta E/E$ x 10^{-4}
1	4A	perfect crystal				1.9	77	1	1.2
2	4C2	annealed for 24 hours at 780ºC	7.58×10^3	20	24	5.4	51	2.98	3.4
3	1C2	annealed for 24 hours at 780ºC & 12 hours at 1000ºC	2.88×10^3	20	28	7.8	40	3.19	4.9
4	1B2	annealed for 24 hours at 780ºC & 12 hours at 1170ºC	5.48×10^3	25	18	6.9	49	2.73	4.4
5	1A3	polished (No. 2000)				9.9	50	5.30	6.3
6	1A1	polished (No. 1000)				12.3	45	6.32	7.8
7	1A2	polished (No. 600)				18.7	40	8.22	11.9

(a) 780 °C (b) 1000 °C (c) 1170 °C
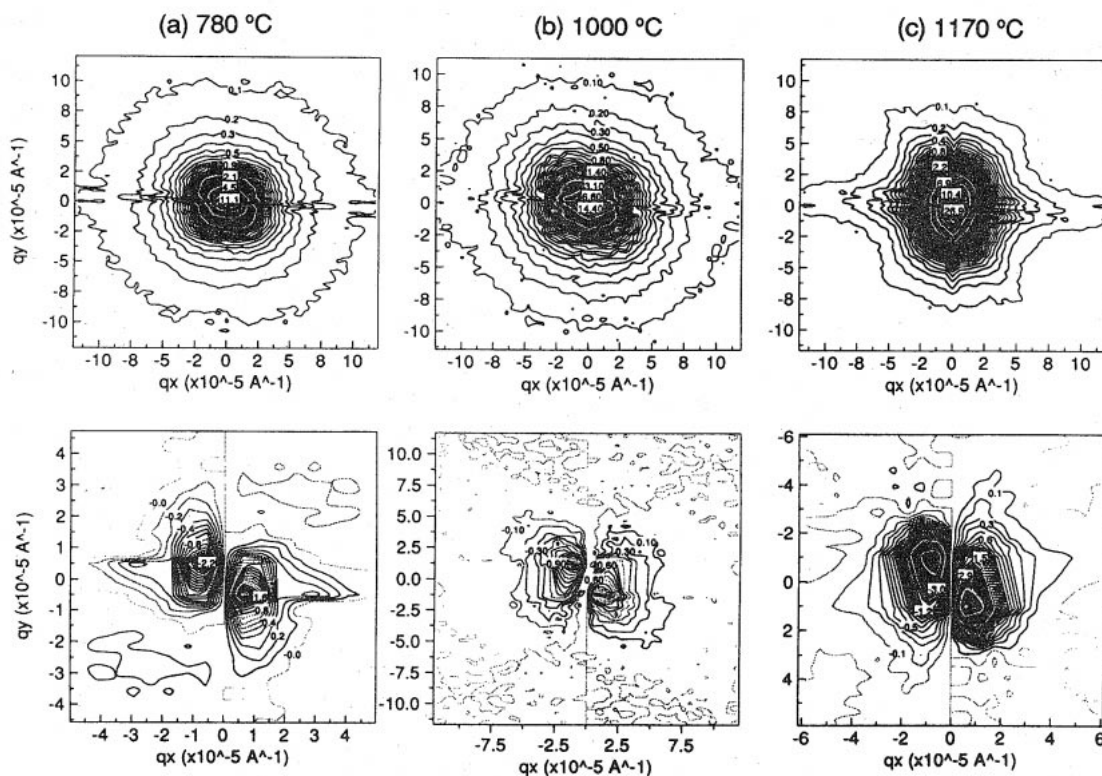
Figure 1 Contours of symmetrical (upper panels) and antisymmetrical (lower panels) parts for the crystals annealed at 780ºC, 1000ºC and 1170ºC, respectively. The every level change in the contour lines is 0.1. The central part is gray due to high line density. Note that the scales of q_x and q_y axes for the symmetrical part are the same but for the antisymmetrical part they are different.

(a) #2000 (b) #1000 (c) #600
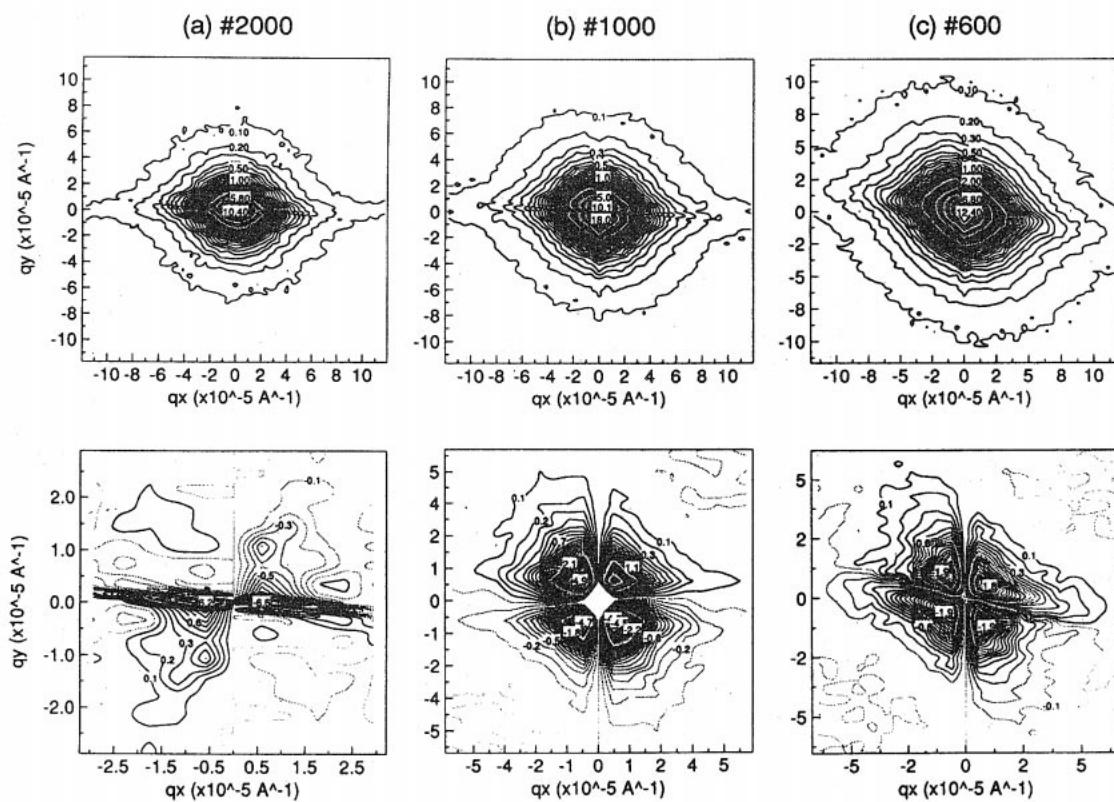
Figure 2 Contours of symmetrical (upper panels) and antisymmetrical (lower panels) parts for the crystals polished with the No. 2000, No. 1000, and No. 600 particles, respectively. The every level change in the contour lines is 0.1. Note that the scales of q_x and q_y axes for the symmetrical part are the same but for the antisymmetrical part they are different.